

Synchronization study in ring-like and grid-like neuronal networks

Jingyi Qu · Rubin Wang · Ying Du ·
Jianting Cao

Received: 13 January 2011/Revised: 17 August 2011/Accepted: 30 August 2011/Published online: 13 September 2011
© Springer Science+Business Media B.V. 2011

Abstract In this paper, we study the synchronization status of both two gap-junction coupled neurons and neuronal network with two different network connectivity patterns. One of the network connectivity patterns is a ring-like neuronal network, which only considers nearest-neighbor neurons. The other is a grid-like neuronal network, with all nearest neighbor couplings. We show that by varying some key parameters, such as the coupling strength and the external current injection, the neuronal network will exhibit various patterns of firing synchronization. Different types of firing synchronization are diagnosed by means of a mean field potential, a bifurcation diagram, a correlation coefficient and the ISI-distance method. Numerical simulations demonstrate that the synchronization status of multiple neurons is much dependent on the network patterns, when the number of neurons is the same. It is also demonstrated that the synchronization status of two coupled neurons is similar with the grid-like neuronal network, but differs radically from that of the ring-like neuronal network. These results may be instructive in understanding synchronization transitions in neuronal systems.

Keywords Ring-like and grid-like neuronal network · ISI-distance · Mean field potential · Bifurcation diagram · Correlation coefficient

Introduction

Neuronal synchronization is known to play a crucial role in many physiological functions such as information binding and wake-sleep cycles (Haken 2002; Liu et al. 2011; Sun et al. 2010; Shi et al. 2008). The synchronization of neuronal signal was proposed as one of the mechanisms to transmit and code information in the human brain (Singer 1994; Pikovsky et al. 2001). Hence, the synchronous firing of interconnected neurons has been extensively investigated by means of the theory of nonlinear dynamics. Synchronization of fast-spiking neurons interconnected by GABA-ergic and electrical synapses was investigated by Nomura and his team (Nomura et al. 2003). It was observed that a fast-spiking pair connected by electrical and chemical synapses could achieve both synchronous and asynchronous firing states in a physiologically plausible range of the conductance ratio between electrical and chemical synapses. Sato and Shiino (2007) investigated effects of the width of an action potential on synchronization phenomena using an integrate-and-fire neuron model and a piecewise linear version of the FitzHugh-Nagumo neuron model. It was shown that the duration of the impulse had a critical role in assuring synchronization. Synchronous behavior of two electrically-coupled neurons was investigated by Postnova et al. (2007a). Asynchronous and various synchronous states such as out-of-phase, in-phase and almost in-phase chaotic synchronization were observed using the phase difference method. Simulation results demonstrated that the tuning of neurons coupling strength could have significant impact on the synchronous states, especially at tonic to bursting transitions (Postnova et al. 2007a).

A variety of measures have been introduced to measure the synchronization transition between two neurons or among multiple neurons. As far as we know, the firing rate and bifurcation diagram are basic and important methods

J. Qu · R. Wang (✉) · Y. Du · J. Cao
Department of Mathematics, Institute for Cognitive
Neurodynamics, School of Science, School of Information
Science and Engineering, East China University of Science and
Technology, Meilong 130, Shanghai 200237, China
e-mail: rbwang@ecust.edu.cn

used to measure spike trains for encoding information in neuroscience (Freeman 2000). Phase differences and phase projection are other common ways to analyze the synchronous state between two coupled neurons (Postnova et al. 2007a). Mean field potential (MFP) is a global parameter for visualization of the network synchronization (Postnova et al. 2010). Since the measures above were all qualitative, the focus of this study lies on those aiming at a quantification of the synchrony degree between two or more spike trains. Prominent examples were cost-based distance introduced by Victor and Purpura (1996), the Euclidean distance proposed in van Rossum (2001), cross correlation of spike trains after filtering (Haas and Write 2002; Schreiber et al. 2003). However, a common property of these methods is the existence of one parameter that sets the time scale. Correlation coefficient has been used to measure the synchronization degree of the two coupled neurons (Wang et al. 2008), which was parameter free and could measure the degree of synchronization quantitatively. However, this method was not suitable for multiple neurons but only two neurons. More recently, a new method ISI-distance has been introduced by Kreuz et al. (2007, 2009), which used the interspike interval (ISI) instead of spike frequency as the basic element of comparison. Since no binning was used, it was both parameter-free and self-adaptive (Du et al. 2010). ISI-distance method was suitable for both two and multiple neurons.

In the present paper, synchronization between two coupled neurons and between multiple neurons with different network connectivity patterns is studied (Wang et al. 2010; Yu et al. 2010; Che et al. 2010; Hao et al. 2010; Ma et al. 2011; Haeri et al. 2010; Gan et al. 2011; Zheng and Lu 2008). There exist different connectivity patterns including ring-like neuronal network and grid-like neuronal network. The former only considers the coupling of nearest neighbor neurons, while the latter includes all the nearest neighbor connected couplings. We are concerned whether the synchronization process has relation with network connectivity patterns. If so, what is the exact difference between them. To give all-sided information about the synchronization, correlation coefficient and ISI-distance methods are adopted to give the quantitative results besides bifurcation diagram to give qualitative analysis. The neuronal network will exhibit various firing synchronization by tuning the key parameters of the coupling strength and the external current injection. We will show that the synchronization depends greatly on the different network connections. The neuron numbers of both the ring-like and the grid-like neuronal networks are the same and as sparse as 25. It is much easier for the grid-like network to reach synchronization than for the ring-like one. More interestingly, the behavior of the two coupled

neurons is much different from the ring-like network while it resembles the grid-like network.

The paper is organized as follows: “**Model**” presents the model equations and network connections, including tonic-to-bursting in a single neuron. “**Results**” presents the main simulation results of two-coupled neurons and neuronal networks with different connection patterns, showing the different states of synchronization by varying control parameters, the coupling strength and external current. Finally, a brief conclusion is given in “**Conclusion**”.

Model

To illustrate what happens when one neuron is coupled with another neuron or when one neuron is in a coupled network, one may employ a dynamical system, consisting of two or more neurons that are coupled via a gap-junctional flux, and study their synchronization properties.

Single neuron pattern generator

Tonic-to-bursting transition seems to be physiologically more relevant in the central nervous system and many neurons can display transitions between tonic spiking and bursting as a function of the brain state (Postnova et al. 2007a, b; Shilnikov and Calabrese 2005b). It have been observed in many models such as Hindmarsh-Rose model (Wang 1993), models of heart interneurons (Shilnikov and Cymbalyuk 2005a) and β -cells model (De Vries and Sherman 2001) etc. In this paper, a modified version of Hodgkin-Huxley approach (Hodgkin and Huxley 1952), the so-called Huber-Braun model is adopted (Finke et al. 2008; Postnova et al. 2010). This model has originally been developed to mimic the temperature dependent alterations of static impulse patterns of peripheral neurons in the skin, which shows pacemaker-like tonic firing, bursting and a broad range of chaos in between (Braun et al. 2000, 2001, 2003; Huber et al. 2006, 2007).

The resultant dynamics of a single neuron are described by the following differential equations:

$$C_M \frac{dV}{dt} = - \sum_i I_i = -I_l - I_d - I_r - I_{sd} - I_{sr} - I_{ext} - I_{couple}, \quad (1)$$

$$I_l = g_l(V - V_l), \quad (2)$$

$$I_i = \rho g_i a_i (V - V_i) \quad i = d, r, sd, sr, \quad (3)$$

$$a_{i\infty} = \frac{1}{1 + \exp(-s_i(V - V_{0i}))} \quad i = d, r, sd, \quad (4)$$

$$\frac{da_i}{dt} = \frac{\phi}{\tau_i} (a_{i\infty} - a_i) \quad i = r, sd, \quad (5)$$

$$a_d = a_{d\infty}, \tag{6}$$

$$\frac{da_{sr}}{dt} = \frac{\phi}{\tau_{sr}} (\eta I_{sd} - ka_{sr}), \tag{7}$$

$$\phi = 3.0^{(T-T_0)/10^\circ C}, \tag{8}$$

$$\rho = 1.3^{(T-T_0)/10^\circ C}, \tag{9}$$

where C_M is the membrane capacitance, V is the membrane voltage, I_d is the depolarizing sodium current, I_r is the repolarizing potassium current, I_{sd} is a slow depolarizing current, a persistent sodium current as well as a low voltage activated calcium current, I_{sr} is a slow repolarizing current, represented as a simplified version of Ca-dependent K-current, I_{ext} accounts for an external current, I_{couple} stands for neighbor gap-junction coupling, g_l is the leak conductance, V_l is the equilibrium potential, g_i is the maximum conductances, a_i is the activation parameters, ρ is used for the temperature scaling of the ion currents, V_{0i} are the half-activation potentials, and s_i the slopes of the steady state activation curves, η is the coupling contrast and k is a relaxation factor.

The numerical parameter values are: equilibrium potential ($V_{sd} = V_d = 50$ mV, $V_{sr} = V_r = -90$ mV, $V_l = -60$ mV); ionic conductances ($g_l = 0.1$, $g_d = 1.5$, $g_r = 2.0$, $g_{sd} = 0.25$, $g_{sr} = 0.4$); membrane capacitance ($C_M = 1$); activation time constants ($\tau_r = 2$ ms, $\tau_{sd} = 10$ ms, $\tau_{sr} = 20$ ms); slope of steady state activation ($s_d = s_r = 0.25$ ms, $s_{sd} = 0.09$ ms); half activation potentials ($V_{0d} = V_{0r} = -25$ mV, $V_{0sd} = -40$ mV); coupling and relaxation constants for I_{sr} ($\eta = 0.012$, $k = 0.17$); reference temperature ($T_0 = 25^\circ C$); temperature is set as a constant ($T = 6^\circ C$).

We use I_{ext} in Eq. 1 as a control parameter for tuning the model to different dynamic states. Without an external current ($I_{ext} = 0$ $\mu A/cm^2$), the uncoupled model neuron ($g_c = 0$ ms/cm²) operates in a pacemaker-like tonic firing mode (Fig. 1b). As I_{ext} increases ($I_{ext} = 0.3$ $\mu A/cm^2$), a cascade of period-doubling bifurcations leads to chaotic dynamics (Fig. 1c). With further increasing of current, at ($I_{ext} = 0.6$ $\mu A/cm^2$), the pattern changes to regular burst discharges (Fig. 1d).

Network simulations

Both two reciprocally gap-junction coupled neurons and a neuronal network are simulated in this paper.

For bidirectional coupling of two neurons (Fig. 2a), I_{couple} has the form

$$I_{couple}(i) = g_c(V_i - V_j) \quad i, j = 1, 2 \tag{10}$$

For the ring-like network with N neurons (Fig. 2b), the coupling current $I_{couple}(i)$ is the sum of the previous and next neurons. The closed borders replace $i - 1 = 0$ by $i - 1 = N$, $i + 1 = N + 1$ by $i + 1 = 1$.

$$I_{couple}(i) = g_c(V_i - V_{i-1}) + g_c(V_i - V_{i+1}) \quad i = 1, 2, \dots, N \tag{11}$$

For the grid-like $N \times N$ network (Fig. 2c), the coupling current $I_{couple}(i, j)$ of a neuron at position (i, j) is the sum of the input currents for the nearest neighbor neurons. The summation is taken over all pairs (m, n) with $m, n \in \{-1, 0, 1\}$. The closed borders replace $i + n = 0$ by $i + n = N$, $j + m = 0$ by $j + m = N$, $i + n = N + 1$ by $i + n = 1$, $j + m = N + 1$ by $j + m = 1$.

$$I_{couple}(i, j) = \sum g_c(V_{i,j} - V_{i+n,j+m}) \quad i, j = 1, 2, \dots, N \tag{12}$$

Results

In this section, numerical results of synchronization status between two coupled neurons will be presented firstly. Then, synchronization status of gap-junction coupled ring-like network and grid-like one are simulated, respectively.

Synchronization of two reciprocally gap-junction coupled neurons

A correlation coefficient (CC) has been introduced in (Wang et al. 2008) to measure the synchronization degree of two coupled neurons, the CC is calculated as follows:

$$CC = \frac{\sum_{m=1}^N |V_1^m - \langle V_1^m \rangle| |V_2^m - \langle V_2^m \rangle|}{\sqrt{\sum_{m=1}^N (V_1^m - \langle V_1^m \rangle)^2 \sum_{m=1}^N (V_2^m - \langle V_2^m \rangle)^2}}, \tag{13}$$

where V_1^m (or V_2^m) represents the sampling of the membrane potential $V_1(t)$ (or $V_2(t)$). $\langle \cdot \rangle$ denotes the average over the number of the sampling. N is the sampling number. It is easy to see that the more synchronous the coupled neurons are, the larger the correlation coefficient is, and the complete synchronization state of the coupled neurons is achieved when correlation coefficient is equal to 1.

The bivariate ISI-distance method proposed by Kreuz et al. (2007) is another method to estimate the degree of synchrony between two spike trains. It is a simple complementary approach that extracts information from the interspike intervals by evaluating the ratio of the instantaneous firing rates. This method is parameter free, time scale independent and easy to visualize. We take the instantaneous ISI-ratio between two interspike intervals x_{isi}^1 and x_{isi}^2 , and normalize it. The quantity of ISI-ratio $I_{1,2}(t)$ becomes zero in case of two spike trains are same and approaches -1 and 1 respectively if the first spike train is much higher or lower than the second spike train. In order to derive the distance between two spike trains, the

Fig. 1 **a** Bifurcation diagram of interspike-intervals for a single neuron with tuning of external current. **b–d** Show tonic firing ($I_{ext} = 0 \mu\text{A}/\text{cm}^2$), chaos ($I_{ext} = 0.3 \mu\text{A}/\text{cm}^2$) and bursting regimes ($I_{ext} = 0.6 \mu\text{A}/\text{cm}^2$)

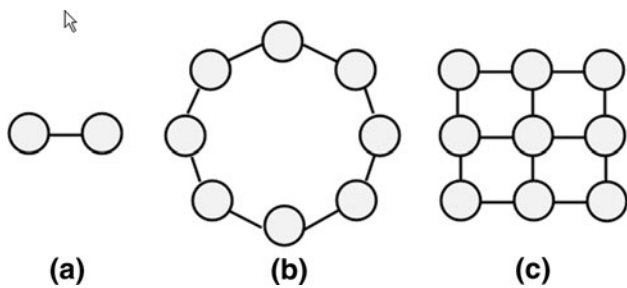
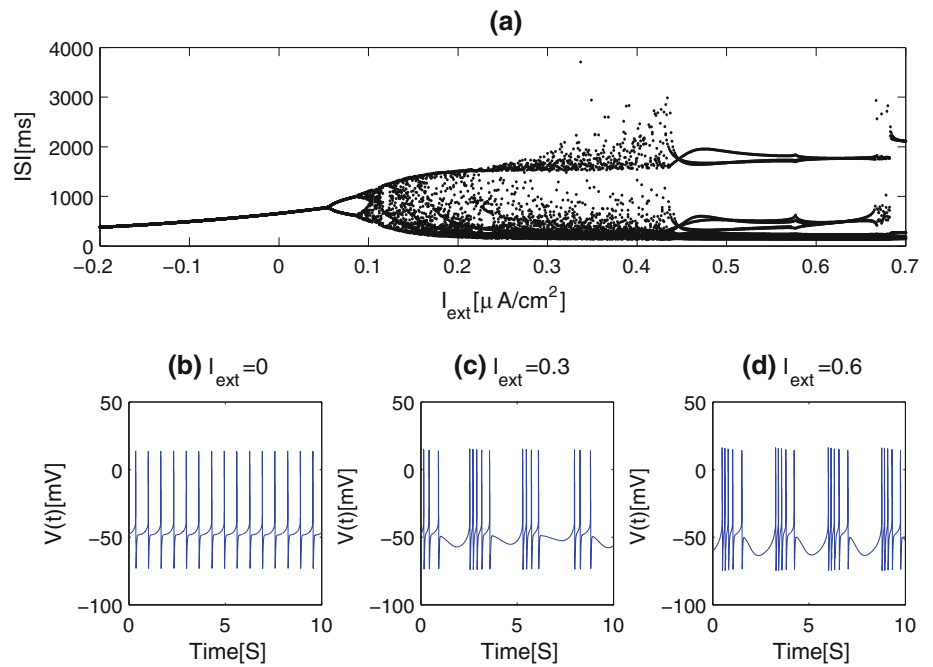


Fig. 2 Schematics of network connectivity patterns. **a** Two reciprocally gap-junction coupled neurons **b** A Gap-junction coupled ring-like neuronal network **c** a gap-junction coupled grid-like neuronal network

absolute ISI-distance D_I is integrated over time. In contrast to the correlation coefficient, the more synchronous the coupled neurons are, the less the bivariate ISI-distance D_I is, and the complete synchronization state of the coupled neurons is achieved when D_I is equal to 0.

$$I_{1,2}(t) = \begin{cases} \frac{x_{isi}^1(t)}{x_{isi}^2(t)} - 1 & x_{isi}^1(t) \leq x_{isi}^2(t) \\ -\left(\frac{x_{isi}^2(t)}{x_{isi}^1(t)} - 1\right) & x_{isi}^1(t) > x_{isi}^2(t) \end{cases} \quad (14)$$

$$D_I = \int_{t=0}^T dt |I(t)| \quad (15)$$

For two reciprocally gap-junction coupled neurons as Fig. 2a, a bifurcation diagram is adopted to give the qualitative analysis while correlation coefficient and bivariate ISI-distance methods are used to give the quantitative results.

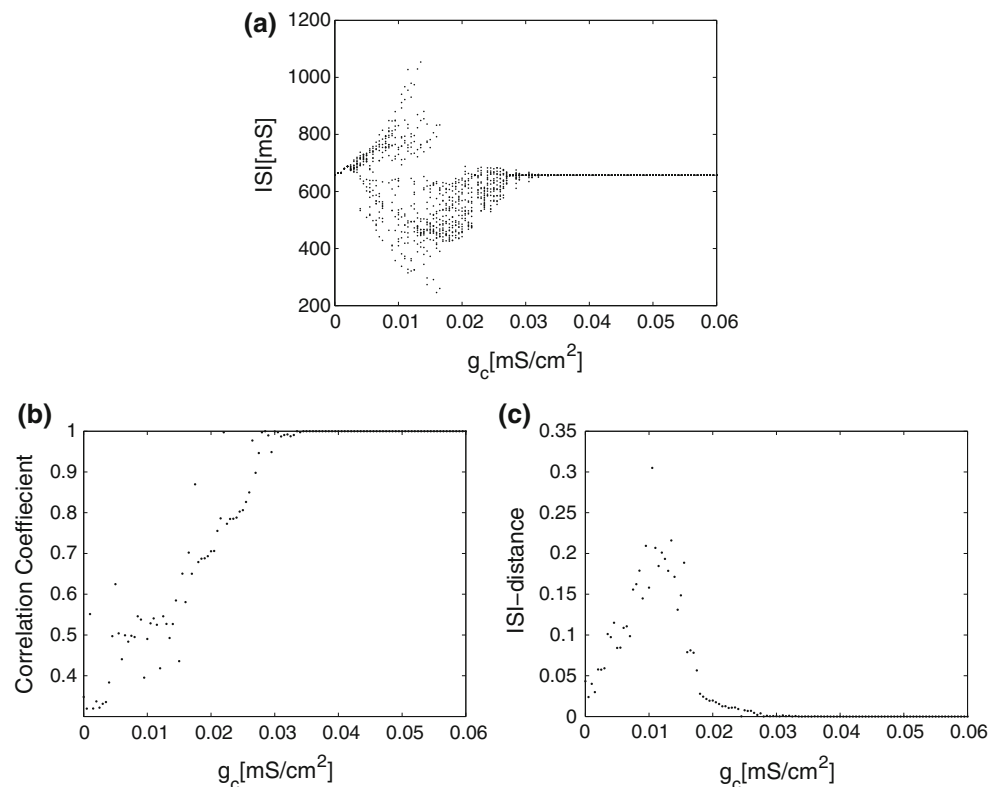
With fixed external current, synchronization of the two coupled neurons are investigated and the numerical results are shown in Figs. 3 and 4 by varying the coupling

strength. In the case of increasing coupling strength we will not only present an example from the tonic firing regime, but also from the bursting regime.

The examples in Fig. 3 are obtained by tuning of the coupling strength in the case when both uncoupled neurons are in the tonic firing regime at a constant value of external current $I_{ext} = 0 \mu\text{A}/\text{cm}^2$. In Fig. 3a the interspike interval bifurcation diagram shows that, as the coupling strength increases, the coupled neurons exhibit complicated firing behaviors, from periodic to chaotic motion firstly, then they go back to tonic firing again when $g_c > 0.03 \text{ mS}/\text{cm}^2$. As illustrated in Fig. 3b, the correlation coefficient value (Eq. 13) increases gradually until it reaches the maximal value 1 and maintains it thereafter. This means that the two neurons become more and more synchronous until they reach a complete synchronous state. Figure 3c shows the change of the bivariate ISI-distance (Eqs. 14, 15) as a function of the increasing coupling strength. It first increases to its maximal value as $g_c < 0.013 \text{ mS}/\text{cm}^2$. The increase of the ISI-distance to its maximal value for $g_c < 0.013 \text{ mS}/\text{cm}^2$ is due to chaotic behavior of the neuron. Then it decreases gradually to 0 in the range of $0.013 < g_c < 0.03 \text{ mS}/\text{cm}^2$. Finally, it stays near 0 as $g_c > 0.03 \text{ mS}/\text{cm}^2$. The ISI-distance shows that the degree of synchronous status initially decreases, then increases until the two neurons are preserved in complete synchronization. Compared with the correlation coefficient, the result of bivariate ISI-distance is more consistent with that of bifurcation diagram.

Compared with Fig. 3, the examples in Fig. 4 are obtained when both uncoupled neurons are in the bursting regime at a constant value of external current $I_{ext} = 0.65 \mu\text{A}/\text{cm}^2$. From the bifurcation diagram of the single neuron in two coupled

Fig. 3 Plots of synchronization status at tonic firing regime ($I_{ext} = 0 \mu\text{A}/\text{cm}^2$) by tuning the coupling strength g_c in two coupled neurons. **a** Bifurcation diagram of a single neuron in two coupled neurons. **b** Plot of correlation coefficient of two coupled neurons. **c** Plot of the ISI-distance of two coupled neurons



neurons (Fig. 4a), it can be seen that the firing pattern of the neuron is always in burst discharges no matter what the value of coupling strength is. The changes in the correlation coefficient and the ISI-distance both show that the two neurons become more and more synchronous ($g_c < 0.02 \text{ mS}/\text{cm}^2$) until they reach the complete synchronous state by tuning the coupling strength.

For a more detailed investigation, the contour graphs of the correlation coefficient and ISI-distance are plotted in the (g_c, I_{ext}) -parameter plane as illustrated in Fig. 5. It can be seen that the correlation coefficient becomes 1 and the ISI-distance becomes 0 in some regions of the parameter, which indicates the realization of complete synchronization between the two coupled neurons. From the maps, one obvious conclusion is that no matter what the I_{ext} is (the uncoupled neurons is in the tonic firing regime, chaotic or bursting status), with increasing the coupling strength, the two coupled neurons can eventually reach the in-phase synchronization.

Synchronization of gap-junction coupled ring-like neuronal network

To compare synchronization effects in larger networks with those in two reciprocally coupled neurons, we couple 25 neurons as ring-like network (Fig. 2b). The coupling

current for each neuron in the network is the sum of the previous and next neurons (Eq. 11).

For multiple neurons, the MFP is adopted as a global parameter for visualization of the synchronization. The MFP is the mean membrane potential of all neurons in the network. Since the most pronounced voltage changes occur during the action potentials, significant MFP deflections can only be expected when a high percentage of the neurons generates action potentials at the same time. The maximum amplitude will only be achieved when all neurons fire in exact coincidence (Postnova et al. 2010). The diagram of ISI which are drawn from a single neuron in the network give some information about the alterations of the impulse patterns. To complement these results, an average bivariate ISI-distance method is introduced to give the quantitative results (Kreuz et al. 2009). We again start by assigning the ISI for each spike train and proceed by calculating the instantaneous average $A(t)$ over all pairwise absolute ISI-ratios $|I_{m,n}(t)|$. Average over time yields D_I^a . It is clear that the more synchronous the multiple spike trains are, the less the average bivariate ISI-distance D_I^a is, and the ideal synchronization state of the neuronal network is achieved when D_I^a is equal to 0.

$$A(t) = \frac{1}{N(N-1)/2} \sum_{n=1}^N \sum_{m=n+1}^N |I_{m,n}(t)| \quad (16)$$

Fig. 4 Plots of synchronization status at bursting firing regime ($I_{ext} = 0.65 \mu\text{A}/\text{cm}^2$) by tuning the coupling strength g_c in two coupled neurons. **a** Bifurcation diagram of the single neuron in two coupled neurons. **b** Plot of correlation coefficient of two coupled neurons. **c** Plot of the ISI-distance of two coupled neurons

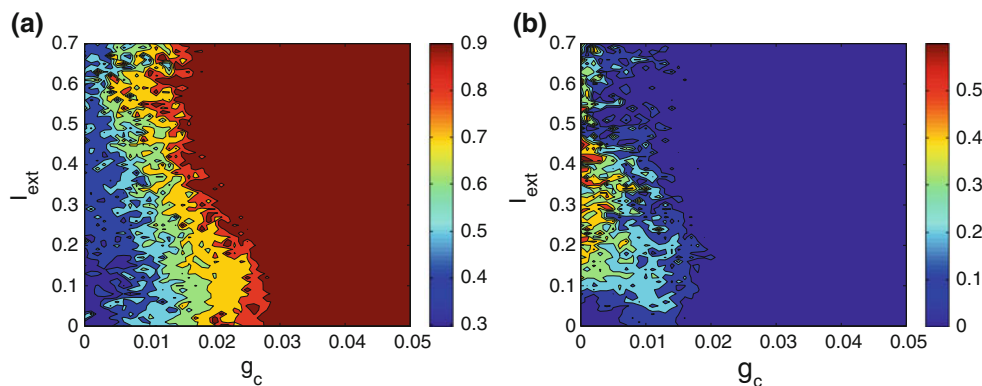
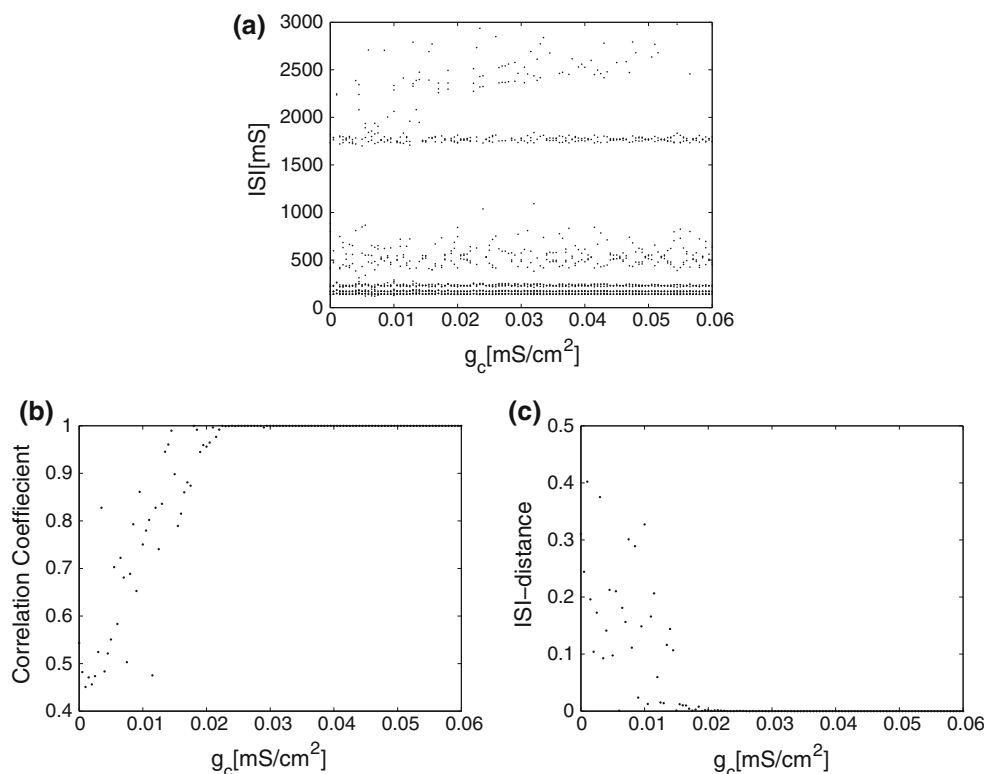


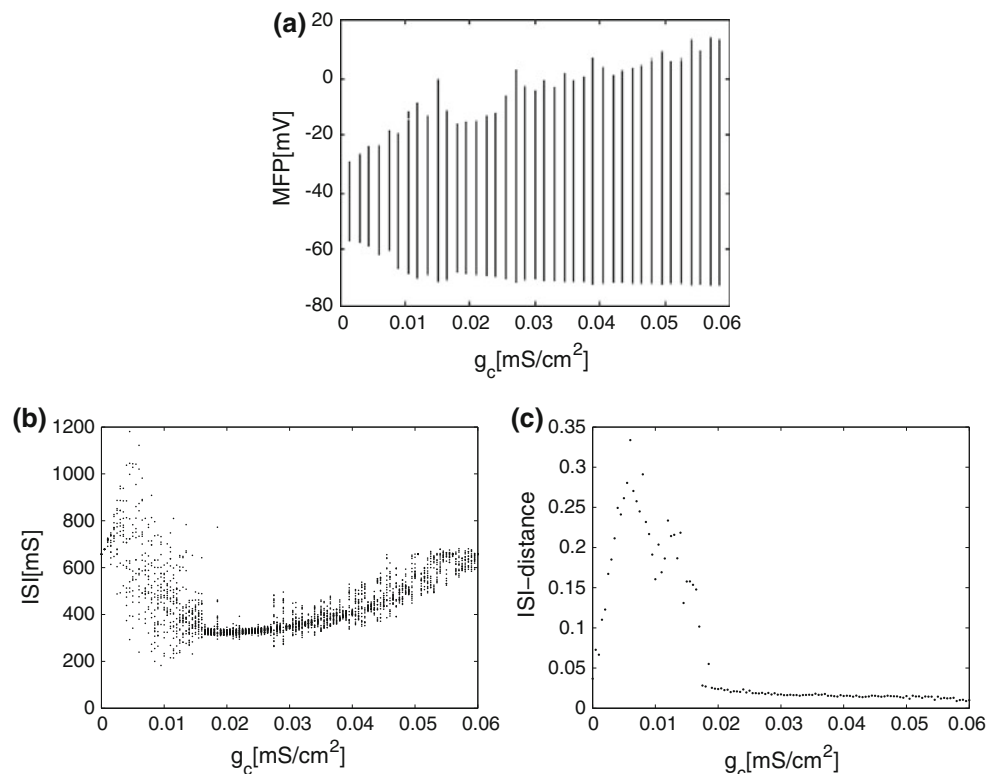
Fig. 5 The contour plot of the ISI-distance in the (g_c, I_{ext}) -parameter plane for two coupled neurons. **a** The contour plot of correlation coefficient. **b** The contour plot of the ISI-distance

$$D_i^a = \frac{1}{T} \int_{t=0}^T A(t) dt \quad (17)$$

In the ring-like tonic firing neuron network ($I_{ext} = 0 \mu\text{A}/\text{cm}^2$), Fig. 6a shows that the transition from the unsynchronized to the synchronized state is not smooth, going in two steps. When coupling strength increases from 0 to $0.017 \text{ mS}/\text{cm}^2$, the deflections of MFP become larger and larger and in a certain rhythm, which indicate that more and more neurons fire simultaneously. When coupling strength is between 0.017 and $0.06 \text{ mS}/\text{cm}^2$, the neurons are in an almost synchronized state, but do not

reach complete synchronization. The corresponding plot of interspike intervals from a single neuron (Fig. 6b) elucidates that coupling values $g_c < 0.017 \text{ mS}/\text{cm}^2$ bring chaotic spike generation. At higher coupling strengths $g_c > 0.017 \text{ mS}/\text{cm}^2$, the neuron goes back to almost tonic firing with a little fluctuation. As to the complementarity of MFP and bifurcation diagram, the plot of average bivariate ISI-distance gives more information. When the coupling strength is small ($g_c < 0.007 \text{ mS}/\text{cm}^2$), the average bivariate ISI-distance increases to 0.3, which means that the degree of synchronous state decreases quickly. However, in the range of $0.007 < g_c < 0.017 \text{ mS}/\text{cm}^2$, the average bivariate ISI-distance decreases to a small

Fig. 6 Plots of synchronization status at tonic firing regime ($I_{ext} = 0 \mu\text{A}/\text{cm}^2$) by tuning the coupling strength g_c in ring-like coupled neurons. **a** Plot of mean field potential (MFP) of ring-like coupled neurons. **b** Bifurcation diagram of the single neuron in ring-like coupled neurons. **c** Plot of the ISI-distance of ring-like coupled neurons



value (almost 0.02) and preserves it, which means the ring-like network is close to synchronous state, but not in complete synchronization.

In a ring-like network of bursting neurons ($I_{ext} = 0.65 \mu\text{A}/\text{cm}^2$), Fig. 7a shows that with increasing coupling strength, the spike-related MFP deflections become larger and larger but with some fluctuations, which means the neurons are more and more synchronous. Synchronization is already complete at about $0.04 \text{ mS}/\text{cm}^2$ where the MFP reaches a plateau. The corresponding plot of interspike intervals from a single neuron (Fig. 7b) shows that no matter what g_c value is, the neuron is always in a bursting state. The value of average bivariate ISI-distance (Fig. 7c) decreases from 0.6 to almost 0 gradually as g_c increases from 0 to $0.04 \text{ mS}/\text{cm}^2$, which means that the synchronous state of ring-like network increases gradually. With further increasing coupling strength, the value of the ISI-distance stays at 0. It means the neuronal network reaches a complete synchronous state. The average bivariate ISI-distance is calculated by Eqs. 16 and 17.

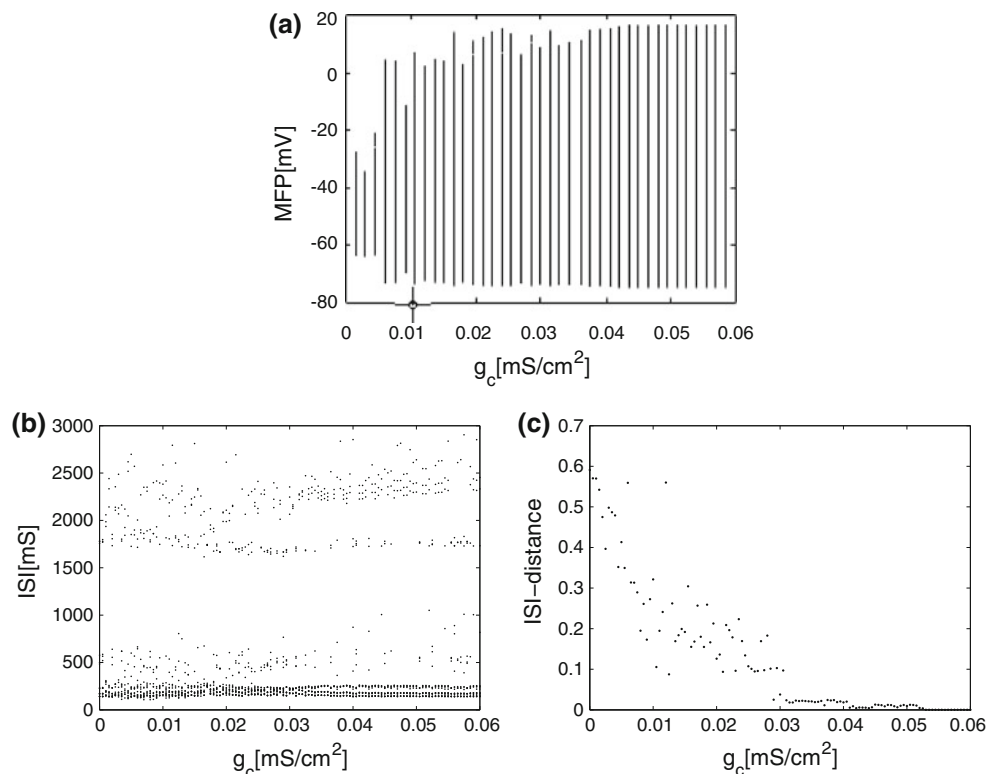
The contour graph of the average bivariate ISI-distance in the (g_c , I_{ext})-parameter plane for the ring-like network is illustrated in Fig. 8. It can be seen that the region that ISI-distance almost equals 0 is much smaller than that of two coupled neurons. It indicates that the realization of synchronization in the 25 coupled ring-like neuron network is much difficult than that of two coupled neurons (Fig. 5b). The plot shows that when coupling strength is bigger than

$0.035 \text{ mS}/\text{cm}^2$, no matter what the value of external current is, the neurons are in a complete synchronous state. Another obvious conclusion is that no matter what the external current is, when increasing the coupling strength, the neurons in the ring-like network can finally reach synchronization. However, when $0.1 < I_{ext} < 0.5 \mu\text{A}/\text{cm}^2$ (the uncoupled neurons display chaotic dynamics, see Fig. 1), the neurons reach the complete synchronization with more difficulty compared with other ranges of $I_{ext} < 0.1 \mu\text{A}/\text{cm}^2$ and $I_{ext} > 0.5 \mu\text{A}/\text{cm}^2$ (the uncoupled neurons is in tonic firing and bursting status, respectively). For example, if $I_{ext} = 0.4 \mu\text{A}/\text{cm}^2$, the neurons can reach the synchronous state only if the values of coupling strength are larger than $0.035 \text{ mS}/\text{cm}^2$. This result reveals that it is more difficult to make the chaotic neurons synchronous than tonic firing and bursting neurons.

Synchronization of a gap-junction coupled grid-like neuronal network

To check whether the synchronization state is related with the network connection patterns or not, we change connectivity pattern from ring-like neuronal network to grid-like one. The number of neurons in the grid-like network (Fig. 2c) is the same as that of the ring-like network, still 25 (5×5). The coupling current of a neuron can be obtained by Eq. 12, which is the sum of the input currents for the nearest neighbor neurons ($M = N = 3$). The

Fig. 7 Plots of synchronization status in the bursting firing regime ($I_{ext} = 0.65 \mu\text{A}/\text{cm}^2$) by tuning the coupling strength g_c in ring-like coupled neuronal network. **a** Plot of mean field potential (MFP) of ring-like coupled neurons. **b** Bifurcation diagram of the single neuron in ring-like coupled neuronal network. **c** Plot of the average bivariate ISI-distance of ring-like coupled neuronal network



neurons at the borders are coupled to the neurons at the opposite border which gives a closed, torus-like network (See “Model”).

In the grid-like tonic firing neuron network ($I_{ext} = 0 \mu\text{A}/\text{cm}^2$), Fig. 9a shows that the values of MFP increase from -30 to 15 mV linearly with increasing coupling strength from 0 to 0.017 mS/cm². With further increasing coupling strength, the MFP reaches the maximum 15 mV and remains there, which means that the synchronization is already complete. The corresponding plot of interspike

intervals from a single neuron (Fig. 9b) elucidates that when coupling values $g_c < 0.017$ mS/cm², the neuron is in a chaotic state. At higher coupling strengths $g_c > 0.017$ mS/cm², the neuron goes back to tonic firing. The plot of average bivariate ISI-distance gives more information. When coupling strength is small ($g_c < 0.01$ mS/cm²), the average bivariate ISI-distance increases to 0.3 , which means the degree of synchronous state decreases. In the range of $0.01 < g_c < 0.017$ mS/cm², the average bivariate ISI-distance decreases to a small value and never changes, which means that the grid-like network is close to the synchronization state. Comparing this result with that of the ring-like network (Fig. 6), there exists two obvious differences. One is that the smaller coupling strength 0.017 mS/cm² can drive the tonic firing of the grid-like network back to the complete synchronous state while it can only go to an almost synchronous state for the ring-like neuronal network. The other difference is that the tonic firing of the grid-like network has less fluctuations than that of the ring-like network, which can be measured by both a plot of mean field potential and bifurcation diagram of the single neuron.

In a grid-like network of bursting neurons ($I_{ext} = 0.65 \mu\text{A}/\text{cm}^2$), Fig. 10a shows that the values of MFP increase from -30 mV to almost 15 mV linearly and remains there with increasing coupling strength. The MFP reaches the maximum when coupling strength reaches 0.01 mS/cm², which is smaller than 0.017 mS/cm² for tonic firing neurons (Fig. 9a). It indicates that for grid-like

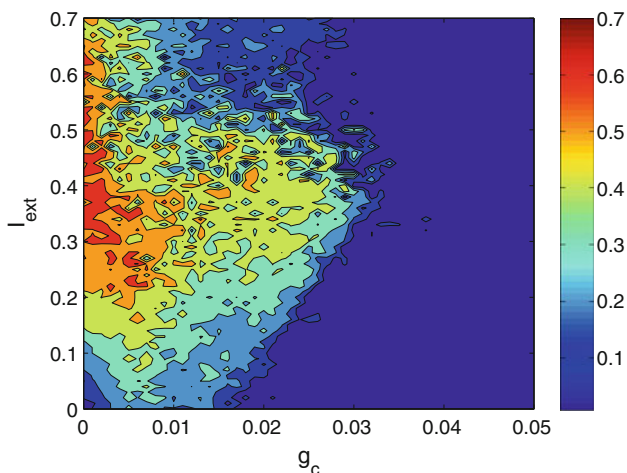
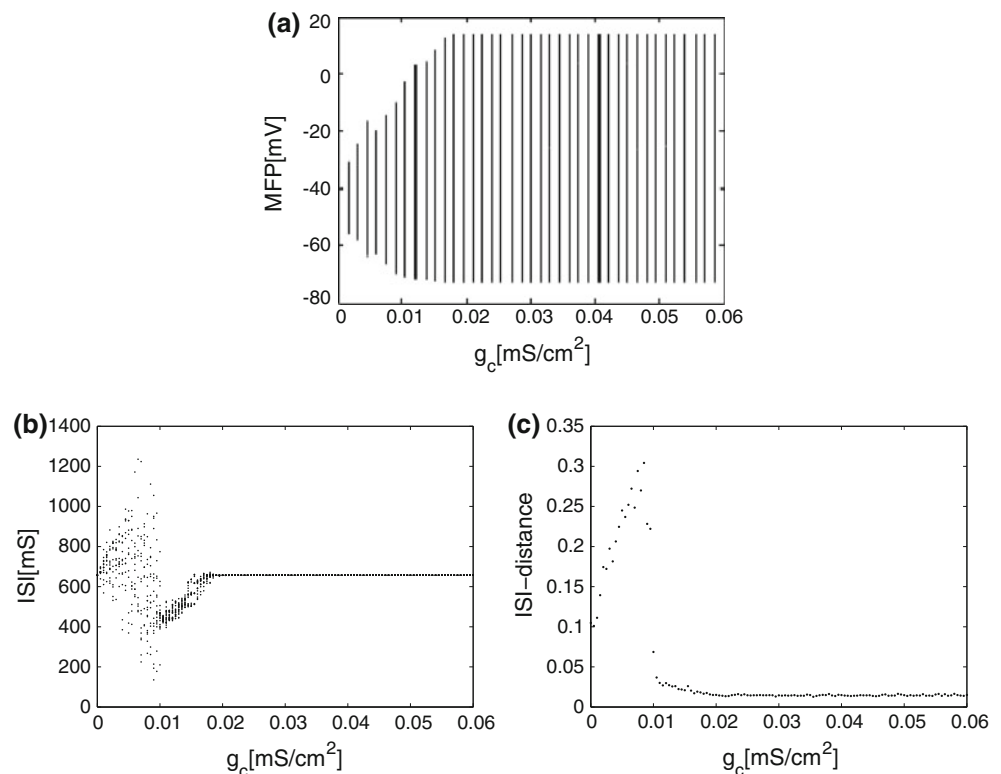


Fig. 8 The contour plot of the average bivariate ISI-distance in the (g_c , I_{ext})-parameter plane for ring-like network

Fig. 9 Plots of synchronization status at tonic firing regime ($I_{ext} = 0 \mu\text{A}/\text{cm}^2$) by tuning the coupling strength g_c in grid-like neuronal network. **a** Plot of mean field potential (MFP) of grid-like neuronal network. **b** Bifurcation diagram of the single neuron in grid-like neuronal network. **c** Plot of the average bivariate ISI-distance of grid-like neuronal network



network, the neurons in the bursting regime reach the complete synchronization easier than those in tonic firing regime. The corresponding plot of interspike intervals from a single neuron (Fig. 10b) shows that no matter what g_c is, the neurons always in bursting state, the ISI value is similar with that of two coupled neurons. As $g_c < 0.01 \text{ mS}/\text{cm}^2$, the value of ISI-distance (Fig. 10c) decreases quickly from 0.5 to almost 0, which means the bursting neurons in the grid-like network can easily reach the synchronous state compared with both ring-like network (Fig. 7c) and two coupled neurons (Fig. 4c).

The contour graph of the average bivariate ISI-distance in the (g_c, I_{ext}) -parameter plane for the grid-like network is illustrated in Fig. 11. The map is similar with that of two coupled neurons (Fig. 5b) and differs from that of the ring-like neuronal network (Fig. 8). It can be observed that the region that ISI-distance almost equals 0 is much larger than that of the ring-like neuronal network. It indicates that the realization of synchronization in the 25 coupled grid-like neuronal network is much easier than for 25 coupled ring-like neuron network neurons (Fig. 8). It demonstrates that synchronization status is much related to the network connectivity patterns. No matter what the I_{ext} is (the uncoupled neurons is in tonic firing regime, chaotic or bursting status), with increasing the coupling strength, the grid-like neuronal network can eventually reach the complete synchronization. The plot also reveals that when the coupling strength is larger than about $0.017 \text{ mS}/\text{cm}^2$, no

matter what the value of external current is, the neurons are all in complete synchronous state.

Conclusion

In this paper, synchronization status of two coupled neurons and multiple coupled neurons with ring-like and grid-like connection network have been investigated. The double or multiple coupled neurons will exhibit periodic and chaotic motions by tuning some key parameters such as the coupling strength and the external current injection.

Three major outcomes are found in this paper. (1) One of them is the demonstration that the synchronization status is much related to the network connectivity patterns in the case where the number of neurons is the same and sparse. The neuron number of both ring-like and grid-like neuronal networks is 25. Large-scale networks have not been simulated yet due to the limitation of computer performance in our lab. By tuning both external current and coupling strength, there exists a larger synchronous region for grid-like neuronal network than that of ring-like network. The former is located at most of the region where coupling strength is larger than $0.017 \text{ mS}/\text{cm}^2$ while the latter is only located at the region where the coupling strength is larger than $0.035 \text{ mS}/\text{cm}^2$. Comparing the tonic firing neurons in grid-like network with those in the ring-like network, when the neurons are injected into a constant external current ($I_{ext} = 0 \mu\text{A}/\text{cm}^2$), coupling strength

Fig. 10 Plots of synchronization status at bursting firing regime ($I_{ext} = 0.65 \mu\text{A}/\text{cm}^2$) by tuning the coupling strength g_c in grid-like neuronal network. **a** Plot of mean field potential (MFP) of grid-like neuronal network. **b** Bifurcation diagram of the single neuron in grid-like neuronal network. **c** Plot of the average bivariate ISI-distance of grid-like neuronal network

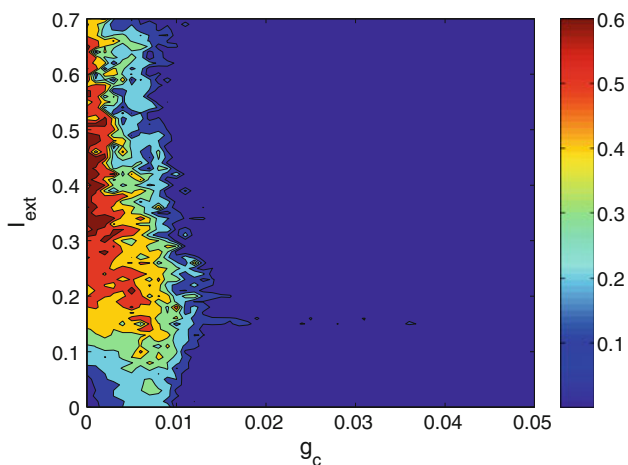
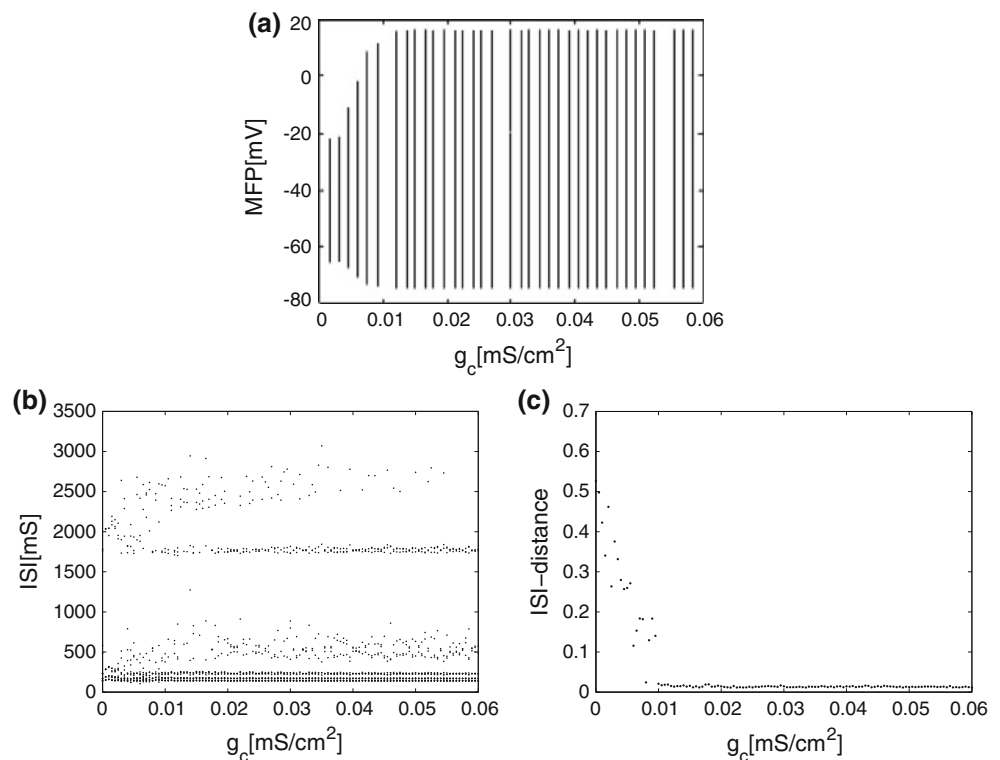


Fig. 11 The contour plot of the ISI-distance in the (g_c, I_{ext}) -parameter plane for grid-like network

0.017 mS/cm^2 can drive the neurons of the grid-like network back to the complete synchronous state while only almost synchronous state for those of ring-like neuronal network. For the bursting neurons of both networks ($I_{ext} = 0.65 \mu\text{A}/\text{cm}^2$), when increasing the coupling strength, the neurons in the grid-like network reach the complete synchronization state more easily than those in the grid-like network. (2) The second outcome is that the synchronization status of two coupled neurons is similar with grid-like neuronal network and has an obvious difference with that of ring-like neuronal network. The synchronous regions for two coupled neurons and grid-

like neuronal network are similar, which is located at most of the region where coupling strength is bigger than 0.017 mS/cm^2 . (3) Thirdly, the two coupled neurons will immediately synchronize when they discharge in bursts. In contrast, both the ring-like and grid-like networks need a significant coupling strength for complete synchronization also in the bursting regime. The methods and results in this paper provide some guidelines to understanding the collective behavior of gap-coupled tonic and bursting neurons.

Acknowledgements The work is supported by National Natural Science Foundation of China (NSFC) (No.10872068,11002055) and the Fundamental Research Funds for the Central Universities. The authors sincerely thank Kreuz et al. sharing their method and code in their web site and Dr.Braun's sincere help for sharing reference documents to us. The authors also thank the anonymous reviewers for their valuable comments that have led to the present improved version of the original manuscript.

References

- Braun HA, Huber MT, Anthes N, Voigt K, Neiman A, Moss F (2001) Noise induced impulse pattern modifications at different dynamical period-one situations in a computer-model of temperature encoding. *Biosystems* 62:99–112
- Braun HA, Huber MT, Anthes N, Voigt K, Neiman A, Pei X, Moss F (2000) Interactions between slow and fast conductances in the Huber/Braun model of cold receptor discharges. *Neurocomputing* 32(33):61–66
- Braun HA, Schäfer K, Voigt K, Huber MT (2003) Temperature encoding in peripheral cold receptors: oscillations, resonances,

- chaos and noise. *Nonlinear Dyn Spatiotemp Princ Biol* 88(332):293–18
- Che YQ, Wang J, Tsang KM, Chan WL (2010) Unidirectional synchronization for Hindmarsh-Rose neurons via robust adaptive sliding mode control. *Nonlinear Anal Real World Appl* 11:1096–1104
- De Vries G, Sherman A (2001) From spikes to bursters via coupling: help from heterogeneity. *Bull Math Boil* 63:371–391
- Du Y, Lu QS, Wang RB (2010) Using interspike intervals to quantify noise effects on spike trains in temperature encoding neurons. *Cogn Neurodyn* 4:199–206
- Finke C, Vollmer J, Postnova S, Braun HA (2008) Propagation effects of current and conductance noise in a model neuron with subthreshold oscillations. *Math Boisci* 214:109–121
- Freeman WJ (2000) *Neurodynamics—an exploration in mesoscopic brain dynamics*. Springer, London
- Gan QT, Xu R, Kang XB (2011) Synchronization of chaotic neural networks with mixed time delays. *Commun Nonlinear Sci Numer Simulat* 16:966–974
- Haas JS, Write JA (2002) Frequency selectivity of layer II stellate cells in the medial entorhinal cortex. *J Neurophysiol* 88:2422–2429
- Haeri M, Dehghani M (2010) Modified impulsive synchronization of hyperchaotic systems. *Commun Nonlinear Sci Numer Simulat* 15:728–740
- Haken H (2002) *Brain dynamics—synchronization and activity patterns in pulse-coupled neural nets with delays and noise*. Springer, Berlin
- Hao YB, Gong YB, Lin X, Xie YH, Ma XG (2010) Transition and enhancement of synchronization by time delays in stochastic Hodgkin-Huxley neuron networks. *Neurocomputing* 73:2998–3004
- Hodgkin AL, Huxley AF (1952) A qualitative description of membrane current and its application to conduction and excitation in nerve. *J Physiol* 117:500–544
- Huber MT, Braun HA (2006) Stimulus response curves of a neuronal model for noisy subthreshold oscillations and related spike generation. *Phys Rev E* 73(41929):1–10
- Huber MT, Braun HA (2007) Conductance versus current noise in a neuronal model for noisy subthreshold oscillations and spike generation. *Biosystems* 89(1–3):38–43
- Kreuz T, Chicharro D, Andrzejak RG, Haas JS, Abarbanel HDI (2009) Multiple spike train synchrony. *J Neurosci Meth* 183:287–299
- Kreuz T, Haas JS, Morelli A, Abarbanel HDI, Politi A (2007) Measuring spike train synchrony. *J Neurosci Meth* 165:151–161
- Liu XY, Cao JD (2011) Local synchronization of one-to-one coupled neural networks with discontinuous activations. *Cogn Neurodyn* 5(1):13–20
- Ma J, Li F, Huang L, Jin WY (2011) Complete synchronization, phase synchronization and parameters estimation in a realistic chaotic system. *Commun Nonlinear Sci Numer Simulat* 16:3770–3785
- Nomura M, Fukai T, Aoyagi T (2003) Synchrony of fast-spiking interneurons interconnected by GABAergic and electrical synapses. *Neural Comput* 15:2179–2198
- Pikovsky A, Rosenblum M, Kurths J (2001) *Synchronization, a universal concept in nonlinear sciences*. Cambridge University Press, New York
- Postnova S, Christian F, Jin W, Schneider H, Braun HA (2010) A computational study of the interdependencies between neuronal impulse pattern, noise effects and synchronization. *J Physiol Paris* 104:176–189
- Postnova S, Voigt K, Braun HA (2007) Neural synchronization at tonic-to-bursting transitions. *J Boil Phys* 33:129–143
- Postnova S, Wollweber B, Voigt K, Braun HA (2007) Impulse-pattern in bidirectionally coupled model neurons of different dynamics. *Biosystems* 89(1–3):135–142
- Sato YD, Shiino M (2007) Generalization of coupled spiking models and effects of the width of an action potential on synchronization phenomena. *Phys Rev E* 75:011909–011915
- Schreiber S, Fellous JM, Whitmer JH, Tiesinga PHE, Sejnowski TJ (2003) A new correlation-based measure of spike timing reliability. *Neurocomputing* 52:925–931
- Shi X, Wang QY, Lu QS (2008) Firing synchronization and temporal order in noisy neuronal networks. *Cogn Neurodyn* 2(3):195–206
- Shilnikov A, Cymbalyuk G (2005) Transition between tonic spiking and bursting in a neuron model via the blue-sky catastrophe. *Phys Rev Lett* 94:048101–041930
- Shilnikov A, Calabrese G (2005) Mechanism of bistability: tonic spiking and bursting in a neuron model. *Phys Rev E* 71:056214–056219
- Singer W (1994) *Time as coding space in neocortical processing*. Springer, Berlin
- Sun WG, Wang RB, Wang WX, Cao JT (2010) Analyzing inner and outer synchronization between two coupled discrete-time networks with time delays. *Cogn Neurodyn* 4(3):225–231
- Van Rossum MCW (2001) A novel spike distance. *Neural Comput* 13:751–763
- Victor J, Purpura K (1996) Nature and precision of temporal coding in visual cortex: a metric-space analysis. *J Neurophysiol* 76:1310–1326
- Wang QY, Duan ZS, Feng ZS, Chen GR, Lu QS (2008) Synchronization transition in gap-junction-coupled leech neurons. *Physica A* 387:4404–4410
- Wang QY, Lu QS, Duan ZS (2010) Adaptive lag synchronization in coupled chaotic systems with unidirectional delay feedback. *Int J Non-Linear Mech* 45:640–646
- Wang XJ (1993) of bursting oscillations in the Hindmarsh-Rose model and homoclinicity to a chaotic saddle. *Physica D* 62:263–274
- Yu WW, Cao JD, Lu WL (2010) Synchronization control of switched linearly coupled neural networks with delay. *Neurocomputing* 73:858–866
- Zheng YH, Lu QS (2008) Spatiotemporal patterns and chaotic burst synchronization in a small-world neuronal network. *Physica A* 387:3719–3728